ELSEVIER

Biophysical Chemistry 113 (2005) 145–154

Biophysical Chemistry

www.elsevier.com/locate/bpc

Effects of gap junction to Ca^{2+} and to IP_3 on the synchronization of intercellular calcium oscillations in hepatocytes

Dan Wu*, Ya Jia, Xuan Zhan, Lijian Yang, Quan Liu

Department of Physics and Institute of Biophysics, Central China Normal University, Wuhan 430079, Hubei, China

Received 20 May 2004; received in revised form 2 September 2004; accepted 2 September 2004
Available online 28 September 2004

Abstract

The frequency of free cytosolic calcium concentration ($[Ca^{2+}]$) oscillations elicited by a given agonist concentration differs between individual hepatocytes. However, in multicellular systems of rat hepatocytes and even in the intact liver, $[Ca^{2+}]$ oscillations are synchronized and highly coordinated. In this paper, we have investigated theoretically the gap junction permeable to calcium and to IP_3 on intercellular synchronization by means of a mathematical model, respectively. It is shown that gap junction permeable to calcium and to IP_3 are effective on synchronizing calcium oscillations in coupled hepatocytes. Our theoretical results are similar either for the case of Ca^{2+} acting as coordinating messenger or for the case of IP_3 as coordinating messenger. There exists an optimal coupling strength for a pair of connected hepatocytes. Appropriate coupling strength and IP_3 level can induce various harmonic locking of intercellular $[Ca^{2+}]$ oscillations. Furthermore, a phase diagram in two-dimensional parameter space of the coupling strength and IP_3 level (or the velocity of IP_3 synthesis) has been predicted, in which the synchronization region is similar to Arnol'd tongue.

Keywords: Coupling strength; IP_3 level; Intercellular Ca^{2+} oscillations

1. Introduction

It is well known that biochemical oscillations are encountered at all levels of biological organization, with periods ranging from a fraction of a second to years [1]. Hormone-induced oscillations in intracellular Ca^{2+} concentration have important roles in the physiology of most cell types [2–5]. Isolated hepatocytes, as well as many other cells, exhibit $[Ca^{2+}]$ oscillations upon stimulation with low concentrations of IP_3-dependent agonists [6,7]. $[Ca^{2+}]$ oscillations in hepatocytes play important roles in regulation. For example, Ca^{2+} regulates phosporylation–dephosphorylation cycle process involved in glycogen degradation, which have been investigated theoretically [8,9].

Intracellular wavelike propagation of $[Ca^{2+}]$ oscillations across single cells is driven mainly by a regenerative process of Ca^{2+} release from the endoplasmic reticulum, mediated by IP_3 receptors [10,5]. In the intact liver, Robbgaspers et al. [11] and Nathanson et al. [12] found that calcium oscillations evoked by IP_3-linked agonists are organized as coordinated periodic waves across whole liver lobules (some 500 cells). On the smaller scale of isolated hepatocyte couplets, this coordination manifests itself as near-synchrony of calcium oscillations in adjacent cells [13]. This coordination has been investigated on both experiments [13,14] and theoretics [15–17].

A first paper by Tjordmann et al. [13] studied multicellular systems of rat hepatocytes and confirmed that, first, gap junction coupling is necessary for the coordination of $[Ca^{2+}]$ oscillations between the different cells; second, the presence of hormone at each hepatocyte is required for cell–cell Ca^{2+} signal propagation; third, functional differences between adjacent connected hepatocytes could allow a "pacemaker-like" intercellular spread of Ca^{2+} waves. A

* Corresponding author. Tel.: +86 27 62714728; fax: +86 27 67866070.
E-mail addresses: wud@phy.ccnu.edu.cn (D. Wu), jiay@phy.ccnu.edu.cn (Y. Jia).

0301-4622/$ - see front matter © 2004 Elsevier B.V. All rights reserved.
doi:10.1016/j.bpc.2004.09.001

subsequent paper by the same authors [14] continued these studies, combining single-cell studies with experiments on cell populations isolated from the peripheral (periportal) and central (perivenous) zones of the liver cell plate. They found strong evidence that the sequential pattern of calcium responses to vasopressin in these multicellular rat hepatocytes systems was due to a gradient of cell sensitivity (from cell to cell) for the hormone. The first cell to respond had the greatest sensitivity to the global stimulus, while the last cell to respond had the least sensitivity. Such gradients may impose an orientation on calcium waves in liver cells and provide a "pacemaker-like" mechanism for regulating intercellular communication in the liver.

However, the factors coordinating individual [Ca^{2+}] oscillations between connected cells and propagating intercellular Ca^{2+} waves are not precisely known. Dupont et al. [15] studied a model based on junctional coupling of multiple hepatocytes which differ in their sensitivity to the hormonal stimulus. As a consequence of this difference, the intrinsic frequency of intracellular calcium oscillations also varies from cell to cell. These oscillations are coupled by an intercellular messenger, which could be either Ca^{2+} or IP_3. The model yield intercellular waves that were confirmed experimentally. The authors also presented experimental evidence that the degree of synchronization is greater for the first few spikes, in agreement with the prediction of their model. They also presented evidence that suggested, within the context of their model, that IP_3 diffusion through gap junctions (rather than Ca^{2+} diffusion) plays the dominant role in the synchronization of intercellular spiking.

An alternative model has been proposed by Höfer [16] to explain the experimental results obtained by Tjordmann et al. [13]. Höfer noted that this experiment revealed a rather large variability in oscillator frequency between adjacent cells, which he argued is likely to be of random nature. As a consequence, he studied the possibility that this originates from random variations in the structural properties of cells (cell size, cell shape, or ER content). They also predicted that synchronization of calcium oscillations in heterogeneous cells will occur in a window of coupling strength between 0.04 and 0.2 s^{-1}. In addition, Ca^{2+} was assumed to be the messenger passing through gap junctions. His results were in reasonable agreement with results in Ref. [13].

To obtain a better explanation of the experimental results, Gracheva et al. [17] have studied stochastic versions of the above two models. Their simulation is based on a Monte Carlo method. They found that both stochastic models exhibit baseline fluctuations and variations in the peak heights of [Ca^{2+}], and that for one model, there is a distribution of latency times which is comparable to the experimental observation of spike widths.

Although the above three models are relatively successful, they have limitations. For example, the calcium spikes in Ref. [15] models are extremely sharp, whereas the experimental spikes are broader. Höfer's model predicts more reasonable spike widths, but predicts an intercellular synchronization at low stimulus that seems inconsistent with the experiment in Ref. [17]. Höfer [16] assumed that three gates of each IP_3 receptor are in a quasi-steady state. In addition, the effects of intracellular IP_3 level and of gap junction permeable to IP_3 on the synchronization have not been studied.

It is well known that there are different time scales in the three basic IP_3R channel gating processes, namely, IP_3 regulation, Ca^{2+} activation and Ca^{2+} inactivation, respectively [18,19]. Basing on Höfer's model and considering that the opening and closing of one gate in each IP_3 receptor is much slower than those of the other two gates [19], we employ Li–Rinzel model to describe the receptor flux. In this paper, firstly, we explore theoretically the effects of coupling strength for Ca^{2+} and of the intracellular IP_3 level on the synchronization of a pair of coupled cells. Secondly, based on the assumption that connected hepatocytes differ in their sensitivity to an agonist [15], coordinated Ca^{2+} spiking can be ascribed to the diffusion of small amounts of IP_3 through gap junctions. Therefore, we studied the effects of coupling strength for IP_3 and of the difference in the sensitivity to hormone on the synchronization of a pair of coupled cells. This paper investigates the synchronization of intercellular Ca^{2+} oscillations mainly on the angle of physics.

2. Model

2.1. Model of intracellular Ca^{2+} as a coordinating messenger

Hormone-evoked calcium dynamics in hepatocytes (as in many other cell types) involve the interplay of calcium fluxes from and into the ER and across the plasma membrane and possibly also other compartments such as mitochondria. We aim to analyze the dynamics of coupled cells, so a relatively simple model proposed by Höfer [16] is applied in this paper. Höfer's model involves calcium release fluxes from the ER (denoted by J_{rel}), calcium reuptake through the sarco/endoplasmic reticulum calcium ATPase (SERCA) (denoted by J_{SERCA}), the calcium fluxes across the plasma membrane (denoted by J_{in} and J_{out}), and the gap-junctional flux. Assuming spatial uniformity of the calcium concentration in the cytoplasm and the ER, the balanced equations for the concentration of cytoplasmic-free calcium and the free calcium content of the whole cell in the ith cell (x_i and z_i, respectively) are given by:

$$\frac{dx_i}{dt} = \rho\left(\left(J_{in} - J_{out}\right) + \alpha\left(J_{rel} - J_{SERCA}\right)\right) + \gamma_{CA}\left(x_j - x_i\right), \tag{1}$$

$$\frac{dz_i}{dt} = \rho\left(J_{in} - J_{out}\right) + \gamma_{CA}\left(x_j - x_i\right), \tag{2}$$

the index i, j=1, 2. A conservation of the total cellular Ca^{2+} implies the constraint $z=x+\beta y$. y denotes the free calcium concentration in the ER. ρ, α and β are structural characteristics of cell. γ_{CA} is the junctional coupling strength. If taking γ_{CA}=0, Eqs. (1) and (2) describe the dynamical behavior of isolated cells.

The expressions for these fluxes are:

$$J_{in} = v_0 + v_c \frac{P}{K_0 + P}, \tag{3}$$

$$J_{out} = v_4 \frac{x^2}{K_4^2 + x^2}, \tag{4}$$

$$J_{SERCA} = v_3 \frac{x^2}{K_3^2 + x^2}, \tag{5}$$

$$J_{rel} = \left(k_1 m_\infty^3 n_\infty^3 h^3 + k_2\right)(y - x), \tag{6}$$

this model assumes that three equivalent and independent subunits are involved in conduction in an IP_3R. Each subunit has one IP_3 binding site (m gate), and two Ca^{2+} binding sites [one for activation (n gate), the other for inhibition (h gate)]. Because the IP_3 binding is at lease 200 times faster than the Ca^{2+} activation binding, and the Ca^{2+} activation binding is at least 10 times faster than the Ca^{2+} inactivation binding and the change rate of [Ca^{2+}] during oscillations, the fast variables m and n can be replaced by their quasi-equilibrium values m_∞ and n_∞ [19]:

$$m_\infty = \frac{P}{d_P + P},$$

$$n_\infty = \frac{x}{d_a + x},$$

Höfer 's model assumed that h also to be in a quasi-steady state. However, the opening and closing of h gate in each IP_3 receptor is much slower than those of the other two gates. Moreover, in the present paper, we will study the effects of IP_3 level, which is involved in h gates open rate. Therefore, the balance equation for h is given by [19]:

$$\frac{dh}{dt} = \alpha_h(1 - h) - \beta_h h, \tag{7}$$

with

$$\alpha_h = d_2 \frac{P + d_1}{P + d_3},$$

$$\beta_h = x,$$

α_h and β_h are opening rate and closing rate for h gates, respectively. The values of these parameters [19,16] are: ρ=0.02 μm^{-1}; α=2; β=0.1; v_0=0.2 $\mu M\ s^{-1}$; v_c=4.0 $\mu M\ s^{-1}$; v_3=9.0 $\mu M\ s^{-1}$; v_4=3.6 $\mu M\ s^{-1}$; k_1=40.0 s^{-1}; k_2=0.02 s^{-1}; K_0=4.0 μM; K_3=0.12 μM; K_4=0.12 μM; d_a=0.23 μM; d_p=1.66 μM; d_2=0.6 μM; d_1=0.3 μM; d_3=0.2 μM. To supply the demand of model, we have made a little change to parameters d_a, d_p and d_2. Parameter P is considered as a control parameter, and γ_{CA} is treated as a crucial free parameter.

2.2. Model of intracellular IP_3 as a coordinating messenger

In view of the fact that in the model, IP_3 can diffuse through gap junctions, its progression over time needs to be considered in the description of the Ca^{2+} dynamics in each hepatocyte. To this end, we have incorporated in the model a general equation describing synthesis of IP_3 by phospholipase C (PLC) and IP_3 metabolism by IP_3 3-kinase and 5-phosphatase [20]. The balanced equations for the concentration of intracellular IP_3 in the ith cell (P_i) is given by [15]:

$$\frac{dP_i}{dt} = V_{PLC} - V_K \frac{P_i}{K_K + P_i} \frac{x_i^2}{K_d + x_i^2} - V_{PH} \frac{P_i}{K_{PH} + P_i} + \gamma_{IP}\left(P_j - P_i\right), \tag{8}$$

in this part, Eqs. (1)–(7) remain unchanged, except that γ_{CA} is equal to zero. Therefore, the second model is described by Eqs. (1)–(8). Where V_{PLC} is the velocity of IP_3 synthesis by PLC, which depends on the level of stimulation. V_K and V_{PH} are the maximal velocities of IP_3 metabolism by 3-kinase and 5-phosphatase, respectively. K_K and K_{PH} are the Michaelis constants characterizing the latter enzymes. K_d is the threshold constant for IP_3 3-kinase activation by Ca^{2+}. γ_{IP} is the junctional coupling strength.

The values of these parameters [15] are: V_K=0.075 $\mu M\ s^{-1}$, V_{PH}=0.075 $\mu M\ s^{-1}$, K_K=1.0 μM, K_{PH}=10.0 μM, K_d=0.5 μM. To supply the demand of the model, we have made a change to parameters V_K, d_p and d_2. Parameter V_{PLC} is considered as a control parameter, and IP is treated as a crucial free parameter.

To simulate the effects of the coupling strength and of other factors on the synchronization of intercellular Ca^{2+} oscillations in coupled hepatocytes, Eqs. (1), (2), (7) and (8) were integrated by the forward Euler algorithm with a time step of 0.001 min. In each calculation, the time evolution of the system lasted 1000 min after transient behavior was discarded.

3. Effects of gap junctions on synchronization of intercellular Ca^{2+} oscillations

3.1. Effects of gap junction to Ca^{2+} and of IP_3 level

To investigate the effects of gap junction permeable to Ca^{2+} and of IP_3 level, the model of intracellular Ca^{2+} as a coordinating messenger is applied in this part.

3.1.1. Comparison with experimental results

The calcium dynamics of isolated hepatocytes are well characterized experimentally. There exists a critical

agonist dose above which a hepatocyte responds with regular calcium oscillations. The bifurcation diagram for the intracellular Ca^{2+} concentration in an isolated hepatocyte is plotted in Fig. 1 (the solid line). It is shown that the increase of IP_3 level gives rise to intracellular Ca^{2+} oscillations, and that the average cytosolic Ca^{2+} concentration is increased with the IP_3 stimulation level increasing. At large agonist dose, oscillations disappear again via a second Hopf bifurcation. As known to all, a prominent feature of calcium oscillations in hepatocytes is the encoding of the agonist dose in the frequency of the oscillations. In this model, the frequency of cytosolic calcium oscillations increases greatly with IP_3 level increasing (the figure not shown in this paper). To study the synchronization of intercellular calcium oscillations, a pair of coupled cells are considered. The dashed line in Fig. 1 is the bifurcation diagram for the intracellular Ca^{2+} concentration in one of a pair of coupled hepatocytes. The other cell of the two coupled hepatocytes is set outside oscillation range (subthreshold IP_3 level in this cell). It has been shown that even not in the range of cytosolic Ca^{2+} oscillations for isolated cell, intracellular concentration of calcium for coupled cells can oscillate due to the intercellular calcium communication between coupled cells. The oscillation range for coupled cells is larger than the one for isolated cell. When IP_3 level is high, the cytosolic Ca^{2+} concentration in one of the coupled cells is lower than the Ca^{2+} concentration in isolated cell. This is because cytosolic Ca^{2+} ions in one cell communicate with those in the other cell (in which IP_3 level is relatively low) via a gap junction.

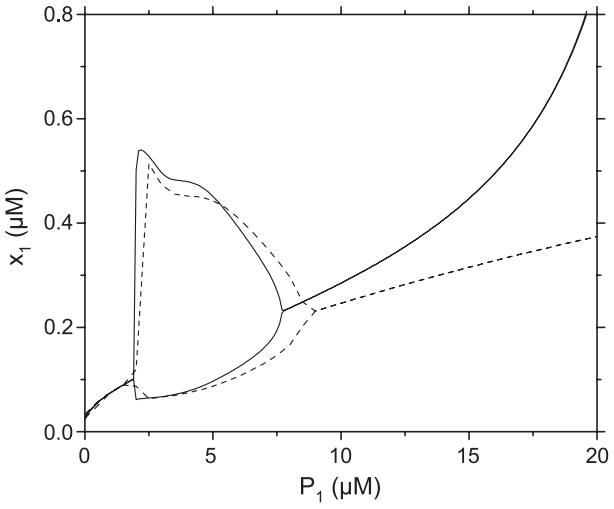

Fig. 1. The bifurcation diagrams of x_1 are plotted against the stimulus parameter, P_1 (IP_3 level in the first cell of two coupled cells). (Solid line: in an isolated hepatocyte; dashed line: in the first cell of two coupled cells.) Within the range of P_1 values giving rise to oscillations, both the maximum and the minimum of x_1 in the course of oscillations are drawn. For the two coupled cells, the coupling strength γ_{CA}=0.02 s^{-1}, and P_2 (IP_3 level in the second cell of the two coupled cells)=1.5 μM.

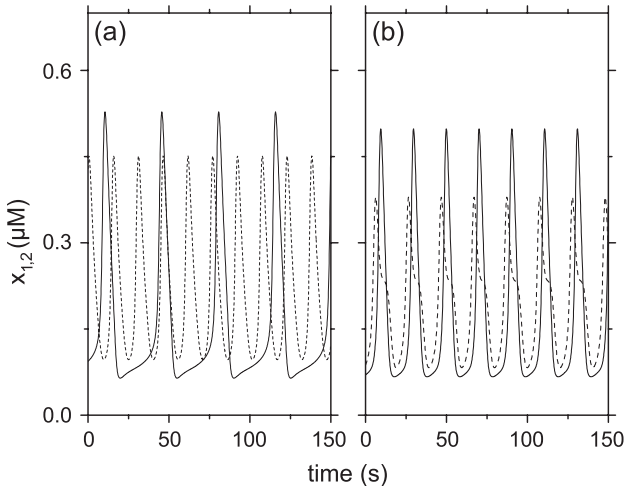

Fig. 2. Time courses of x_1 (solid line) and of x_2 (dashed line) at P_1=2.5 μM and P_2=5.0 μM for different coupling strengths: (a) γ_{CA}=0.0 s^{-1}; (b) γ_{CA}=0.09 s^{-1}.

To investigate the role of gap junction permeable to Ca^{2+} in synchronization of hormone-induced [Ca^{2+}] oscillations, we compare the evolution of x_1 and of x_2 after and before intercellular connection is blocked (Fig. 2). When intercellular connection is blocked (Fig. 2a, γ_{CA}=0 s^{-1}), the cells oscillate at their own intrinsic frequencies, and in general, there is no fixed-phase relation between the cells, which is consistent with the experimental results [21,7]. In Fig. 2a, the intrinsic frequency of x_1 is about 0.028 s^{-1}, and that one of x_2 is about 0.065 s^{-1}. When the gap junction recovers and the coupling strength is big enough (Fig. 2b, γ_{CA}= 0.09 s^{-1}), the cells become synchronous. The frequency of [Ca^{2+}] oscillations for the two cells are both equal to 0.05 s^{-1}. These results suggest that the gap junction is required for the synchronization of hormone-induced cytosolic [Ca^{2+}] oscillations. Furthermore, one cell of the two coupled cells which oscillates quicker seems to impose its frequency on the other cell. This is consistent with the fact that upon coupling of these individual oscillating units, the cell with the highest frequency of oscillation will act as a "pacemaker" for the other cells [13].

In the experiment [13], the authors first stimulated only one of the cells in the doublet with a hormone input (local perfusion). They then stimulated both cells simultaneously (global perfusion). From these studies, they found that local perfusion does not produce Ca^{2+} spiking in the second (unstimulated) cell, while global perfusion of both cells produces well-synchronized [Ca^{2+}] oscillations in the two cells. In Fig. 3a–c, we show our results of stimulating only one cell in the doublet. It is found that the unstimulated cell (in which the IP_3 level is very low) cannot show [Ca^{2+}] oscillations even if we increase the coupling strength to a big enough value (γ_{CA}=0.09 s^{-1}). However, if we stimulate both hepatocytes, they respond with well-coordinated [Ca^{2+}] oscillations (see Fig. 2b). It can be concluded that

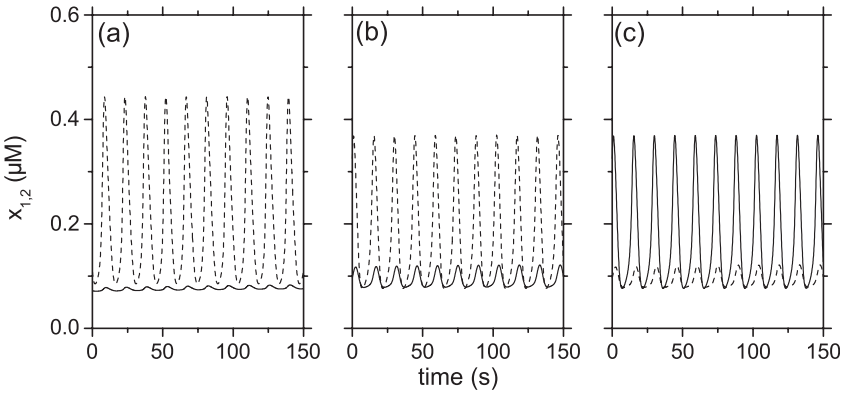

Fig. 3. Time courses of x_1 (solid line) and of x_2 (dashed line). (a) P_1=1.0 μM, P_2=5.0 μM, γ_{CA}=0.02 s^{-1}; (b) P_1=1.0 μM, P_2=5.0 μM, γ_{CA}=0.09 s^{-1}; (c) P_1=5.0 μM, P_2=1.0 μM, γ_{CA}=0.09 s^{-1}.

sufficient IP_3 stimulus is necessary for the synchronization of IP_3-induced [Ca^{2+}] oscillations in coupled hepatocytes.

3.1.2. Phase-locking and harmonic-locking

To make our results more meaningful, we study a pair of coupled cells with P_1=1.5 μM (subthreshold IP_3 level for single cell), and P_2=2.5 μM (above threshold IP_3 level for a single cell). Fig. 4a–c show [Ca^{2+}] oscillations in a pair of coupled cells for three different coupling strength γ_{CA}. Fig. 4a depicts a case of 1:3 harmonic locking. When the strength of coupling increases to a given range, the phases of the two cells become 1:2 harmonic locking (Fig. 4b). Increasing the coupling strength further, the locking ratio gets closer to 1:1, and eventually, the cells become synchronous, i.e., phase locking (Fig. 4c). Höfer [16] depicted a case of 1:2 locking. Furthermore, we have

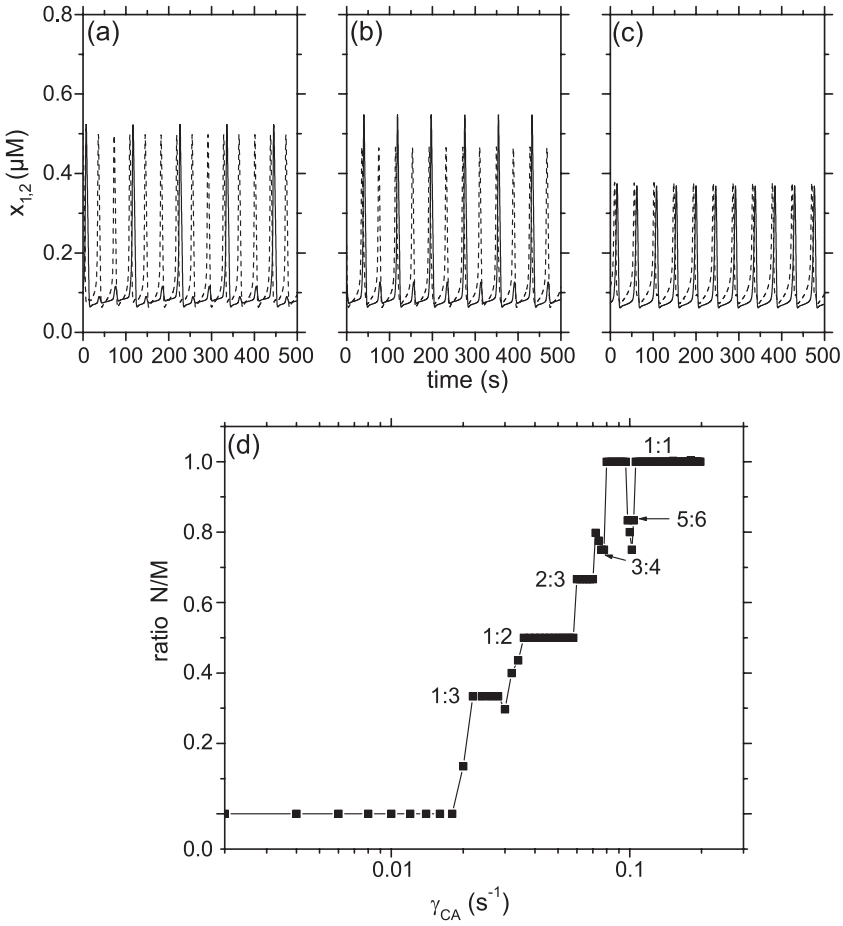

Fig. 4. Time courses of x_1 (solid line) and of x_2 (dashed line) at P_1=1.5 μM and P_2=2.5 μM. (a) Harmonic locking of 1:3 (γ_{CA}=0.025 s^{-1}); (b) harmonic locking of 1:2 (γ_{CA}=0.05 s^{-1}); (c) phase locking of 1:1 (γ_{CA}=0.09 s^{-1}). (d) Devil's staircase, a ratio N/M (where N is the spike number of x_1 and M is the spike number of x_2) as a function of the coupling strength γ_{CA} at given IP_3 level: P_1=1.5 μM, P_2=2.5 μM.

calculated the N/M rhythms as a function of the coupling strength γ_{CA}, where N and M denote the spike number of the [Ca^{2+}] oscillations during an equal long time for the two coupled cells, respectively. It reveals a devil's staircase-like structure as shown in Fig. 4d. The existence of this devil's staircase-like structure with clearly demarcated phase-locked domains is typical of the forced oscillatory dynamics [22]. However, experimentally, this regular ratio of oscillating frequency in coupled cells has not been reported. When coupling strength γ_{CA} is small (smaller than 0.02 s^{-1}), the cell with P_1=1.5 μM cannot show [Ca^{2+}] oscillations, i.e., N=0. Increasing γ_{CA} further leads to the ratio 1:3 rhythm, 1:2, 2:3, 3:4 to the 1:1 rhythm. On the other hand, various rhythms can also be sustained for a range of γ_{CA}. For example, when γ_{CA} is between 0.036 and 0.058 s^{-1}, 1:2 rhythm remains unchanged. In addition, a mysterious well will appear when the coupling strength γ_{CA} is about 0.1 s^{-1}, where the ratio will drop suddenly from 1:1 and will uprising to 1:1 very soon. We suppose that at the borders of phase-locking region, fold bifurcations and hysteresis can occur, which might explain the well.

From Figs. 2 and 4, it can be concluded that γ_{CA}=0.09 s^{-1} is a proper coupling strength to produce synchronous [Ca^{2+}] oscillations in two coupled hepatocytes for P_1=1.5 μM and P_2=2.5 μM. However, is it the same for different P_1 and P_2 values? Thus, we have calculated the N/M rhythms as a function of P_1 at γ_{CA}=0.09 s^{-1} (Fig. 5) and have found a devil's staircase-like structure different from Fig. 4. A 1:1 phase locking has been maintained well when P_1 is between 1.5 and 8.5 μM. However, when P_1 is between 9.0 and 10.5 μM, the phases of the two cells become 2:1 harmonic locking. when P_1 is above 11.5 μM, the cell denoted by 1 cannot show oscillation again. We can predict from Figs. 4 and 5 that, besides γ_{CA}, the IP_3 level in coupled cells plays an important role in the synchronization of intercellular [Ca^{2+}] oscillations.

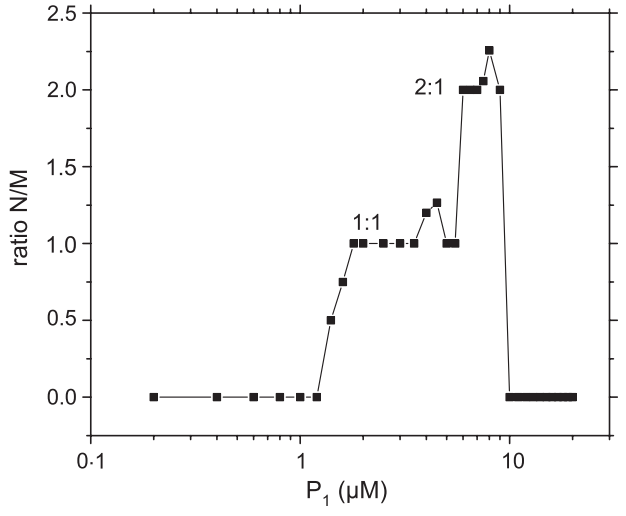

Fig. 5. Devil's staircase, a ratio N/M as a function of P_1. γ_{CA}=0.06 s^{-1}, P_2=20.5 μM.

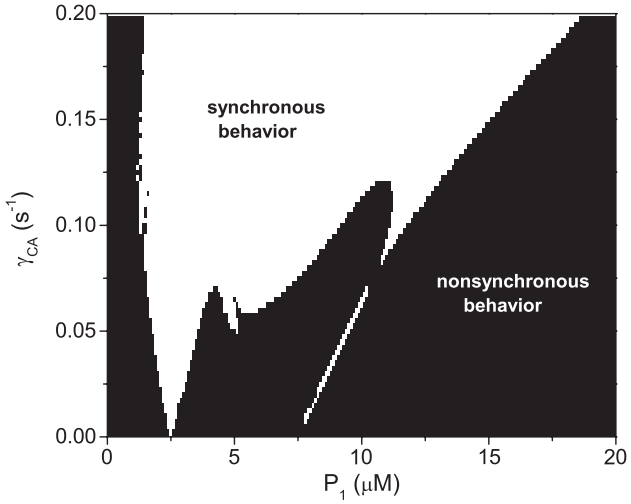

Fig. 6. The synchronization region in P_1–γ_{CA} plane for two coupled hepatocytes. P_2=2.5 μM.

3.1.3. Phase analysis of coupled hepatocytes

From above analysis, we can conclude that both the coupling strength and the IP_3 level play important roles in the coordination of coupled cells. Therefore, in Fig. 6, we plot the phase diagram in two-dimensional parameter space of the coupling strength γ_{CA} and P_1, which provides us an alternative diagnosis of synchronization. The synchronization region similar to Arnol'd tongue obtained by the condition of the total spike number $|N-M|\leq 1$ after time course of 10^4 min. The whitened region corresponds to synchronous behavior, while the shaded region corresponds to nonsynchronous behavior. In Fig. 6, there are two Arnol'd tongue-like structures, one emerging at P_1=2.5 μM and another near 6.0 μM. It can be concluded that the first tongue corresponds to 1:1 locking, and the second one corresponds to the region of 2:1 locking. Fig. 5 can support above conclusion. Arnol'd tongues are generally seen in coupled nonlinear oscillators. For the coupled calcium oscillators, 1:1 tongues were computed in Ref. [16].

3.1.4. Cross-correlation time of coupled oscillators

Another indirect characteristic of the phase locking has been proposed in Ref. [23]. If the phase of a system is locked, the process becomes highly correlated in time.

The cell–cell correlation is defined by the cross-correlation time τ_c [24]:

$$\tau_c = \int_0^{+\infty} d\tau \left(\frac{\langle \tilde{x}_1(t)\tilde{x}_2(t+\tau)\rangle}{(\langle \tilde{x}_1^2\rangle\langle \tilde{x}_2^2\rangle)^{\frac{1}{2}}} \right)^2, \tag{9}$$

with

$$\tilde{x} = x - \langle x \rangle \tag{10}$$

the dependence of the cross-correlation time on the coupling strength and on the IP_3 level are shown in Fig. 7a and b. Both Fig. 7a and b exhibit a maximum. In Fig. 7a, we can observe that the two coupled cells show the strongest

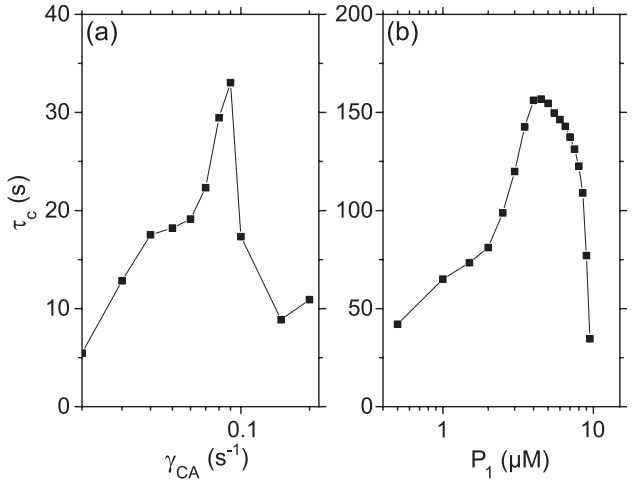

Fig. 7. (a) The cross-correlation time τ_c of two coupled cells vs. the coupling strength γ_{CA} at a given IP_3 level (P_1=1.5 μM, P_2=2.5 μM). (b) The cross-correlation time τ_c of two coupled cells vs. P_1 at γ_{CA}=0.09 s^{-1} and P_2=2.5 μM.

coherence at γ_{CA}=0:09 s^{-1}, which confirms above results in this paper. Fig. 7b demonstrates that when coupling strength is big enough (γ_{CA}=0.09 s^{-1}) and P_2=2.5 μM, the strongest coherence occurs at P_1=4.5 μM.

3.2. Effects of gap junction to IP_3 and of the difference in the sensitivity to hormone

To investigate the effects of gap junction to IP_3 and of the difference in the sensitivity to hormone, the model of intracellular IP_3 as a coordinating messenger is applied in this part. In addition, γ_{CA} is assumed to be zero in this part.

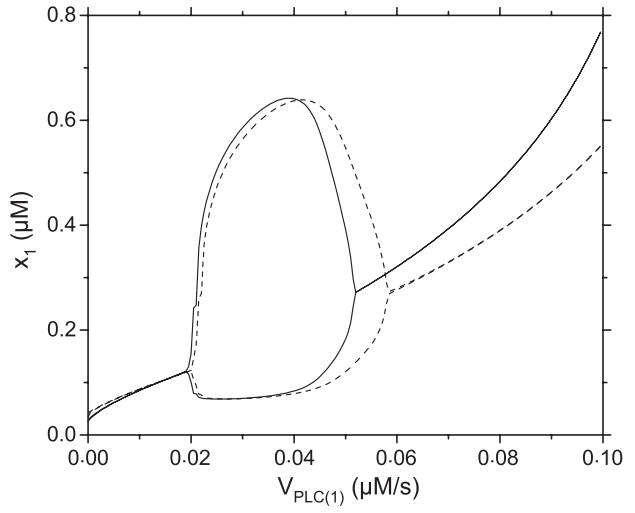

Fig. 8. The bifurcation diagrams of x_1 are plotted against the velocity of IP_3 synthesis in the first cell, $V_{PLC(1)}$. (Solid line: in an isolated hepatocyte; dashed line: in the first cell of two coupled cells.) Within the range of $V_{PLC(1)}$ values giving rise to oscillations, both the maximum and the minimum of x_1 in the course of oscillations are drawn. For the two coupled cells, the coupling strength γ_{IP}=0.01 s^{-1}, and $V_{PLC(2)}$ (V_{PLC} value in the second cell of the two coupled cells)=0.015 μM s^{-1}.

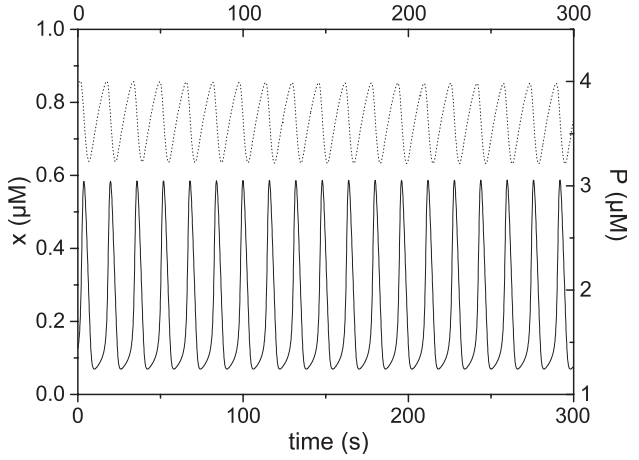

Fig. 9. Time courses of x (solid line, use bottom and left axis) and of P (dashed line, use top and right axis) at $V_{PLC(1)}$=0.03 μM s^{-1} in isolated cell.

It is well known that there is morphological evidence for a gradient of vasopressin receptors along the liver cell plate [25,26]. This increasing density of hormonal receptors from the periportal to the perivenous zones of the liver cell plate may account for a gradient of sensitivity to vasopressin which was observed in Ref. [14]. Indirect evidence suggesting the existence of a similar gradient for α-adrenoceptors has been reported previously [27,14]. Such sensitivity gradients has been taken into account in the model by assuming that each cell has a different velocity of IP_3 synthesis by phospholipase C (V_{PLC}). Therefore, cellular heterogeneity is clearly dominated by these variation in the rate of IP_3 synthesis.

The bifurcation diagrams for the intracellular Ca^{2+} concentration in an isolated hepatocyte (the solid line) and

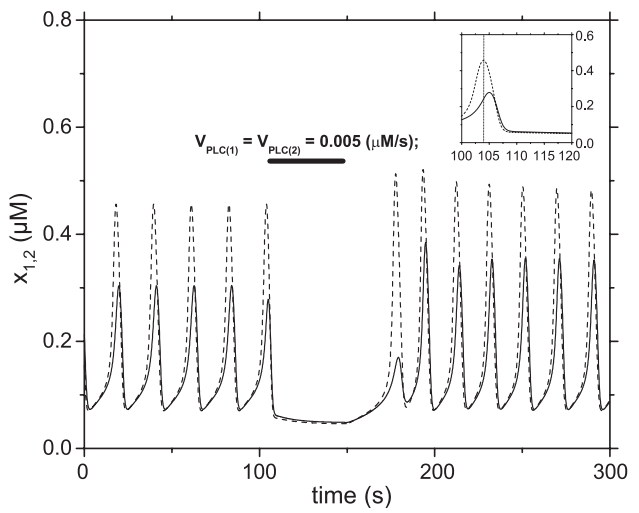

Fig. 10. Time courses of x_1 (solid line) and of x_2 (dashed line) at $V_{PLC(1)}$=0.015 μM s^{-1}, $V_{PLC(2)}$=0.03 μM s^{-1} and γ_{IP}=0.2 s^{-1}. An instantaneous drop of both $V_{PLC(1)}$ and $V_{PLC(2)}$ to a small value 0.005 μM s^{-1} just occurs after the appearance of a Ca^{2+} spike in the first cell. After 50 min, V_{PLC} recovered to $V_{PLC(1)}$=0.015 μM s^{-1} and $V_{PLC(2)}$=0.03 μM s^{-1}. The enlarged inset describes the change in x_1 and x_2 when V_{PLC} drops suddenly.

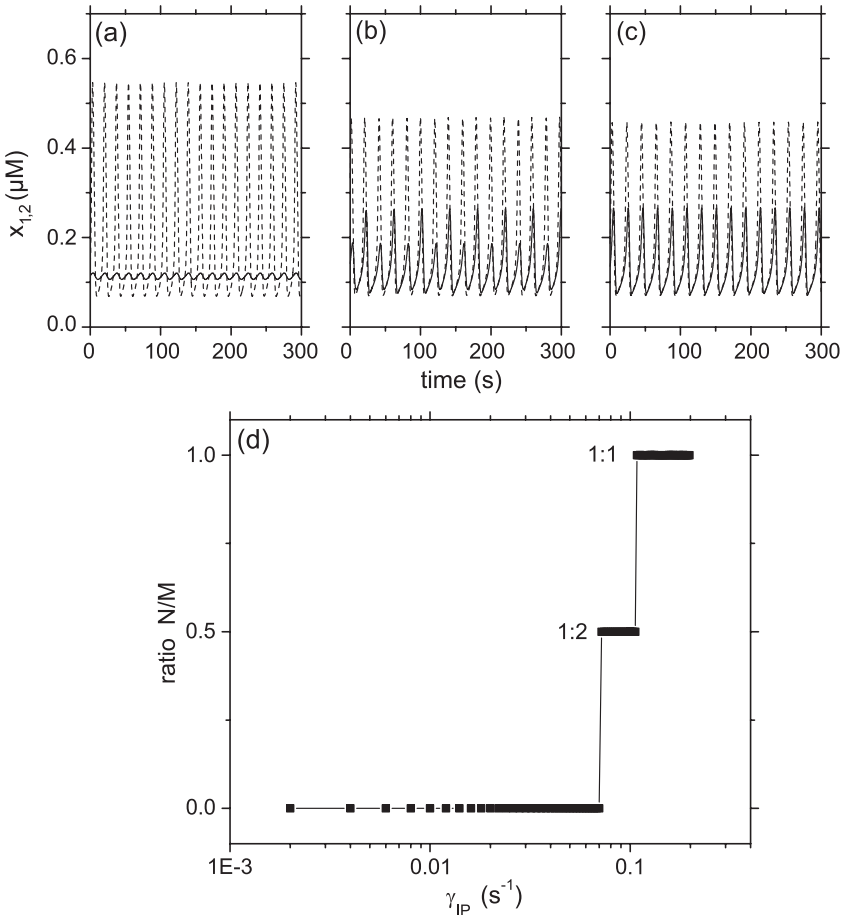

Fig. 11. Time courses of x_1 (solid line) and of x_2 (dashed line) at $V_{PLC(1)}$=0.015 μM s^{-1} and $V_{PLC(2)}$=0.03 μM s^{-1}. (a) Unstimulated (γ_{IP}=0.02 s^{-1}); (b) harmonic locking of 1:2 (γ_{IP}=0.1 s^{-1}); (c) phase locking of 1:1 (γ_{IP}=0.15 s^{-1}). (d) Devil's staircase, a ratio N/M (where N is the spike number of x_1 and M is the spike number of x_2) as a function of γ_{IP}. The velocity of IP_3 synthesis are $V_{PLC(1)}$=0.015 μM s^{-1} and $V_{PLC(2)}$=0.03 μM s^{-1}.

in coupled hepatocytes (the dashed line) has been compared in Fig. 8. The second cell of the two coupled hepatocytes (which is denoted by 2) is set in subthreshold range (near the first Hopf bifurcation). The results in Fig. 8 are similar to those in Fig. 1. Even not in the range of cytosolic Ca^{2+} oscillations for isolated cell, intracellular concentration of calcium for coupled cells can oscillate due to the inter-cellular calcium communication between coupled cells. The oscillation range for coupled cells is larger than the one for isolated cell. To demonstrate the relationship between intracellular [Ca^{2+}] and IP_3 level, their time courses at $V_{PLC(1)}$= 0.03 μM s^{-1} are compared in Fig. 9. The IP_3 level can also oscillate in the range of cytosolic [Ca^{2+}] oscillations (see Fig. 8). Moreover, the intracellular [Ca^{2+}] and IP_3 level oscillate with the same frequency. As can be expected from the regulations considered, the peaks in P precedes the peaks in [Ca^{2+}].

In the discussion that follows, we assume that each cell has a different velocity of IP_3 synthesis (using $V_{PLC(i)}$ to denote the velocity of IP_3 synthesis in the ith cell): $V_{PLC(1)}$=0.015 μM s^{-1} (subthreshold value), $V_{PLC(2)}$=0.03 μM s^{-1} (above threshold value). In Fig. 10, the velocity of IP_3 synthesis has been set at a very low value for a period of time. This corresponds to the agonist being washed out in the experiment. A sudden decrease of V_{PLC} to its basal value in the two coupled cells (at t=104 s) prevented further Ca^{2+}

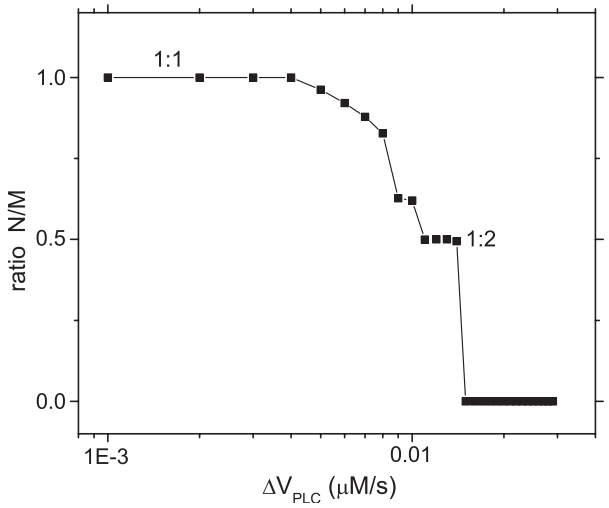

Fig. 12. A ratio N/M as a function of ΔV_{PLC} ($\Delta V_{PLC}=V_{PLC(2)}-V_{PLC(1)}$). $V_{PLC(2)}$=0.03 μM s^{-1} and γ_{IP}=0.05 s^{-1}.

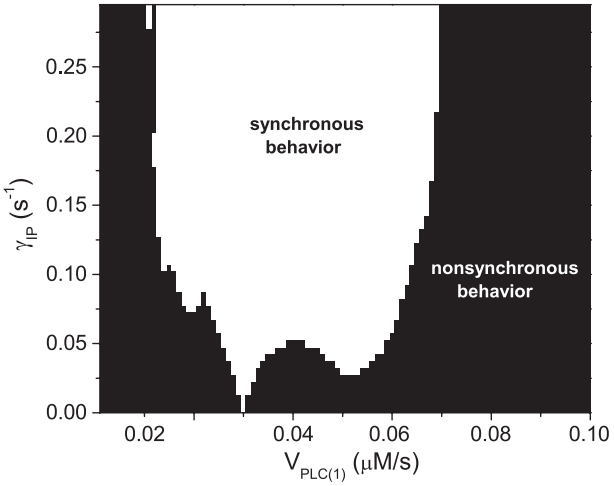

Fig. 13. The synchronization region in $V_{PLC(1)}$–γ_{IP} plane for two coupled hepatocytes. $V_{PLC(2)}$=0.03 μM s^{-1}.

spiking. When V_{PLC} was returned to its original value in the two cells, coordinated Ca^{2+} spiking recovered, similar to that observed in the experiments [15]. It also can be seen that although the decrease of V_{PLC} occurs before the appearance of the Ca^{2+} spike in the second cell (see insert figure in Fig. 10), this Ca^{2+} spike in the second cell can appear because the levels of IP_3 and of Ca^{2+} were already raised before washing.

Fig. 11a–c shows [Ca^{2+}] oscillations in a pair of coupled cells for three different coupling strength γ_{IP}. With the coupling strength γ_{IP} increasing, Fig. 11a–c depicts an unstimulated case, 1:2 harmonic locking and 1:1 phase locking, respectively. Furthermore, we have calculated the N/M rhythms as a function of the coupling strength γ_{IP} in Fig. 11d. It reveals a devil's staircase-like structure, which is simpler than Fig. 4d. When coupling strength γ_{IP} is small (smaller than 0.07 s^{-1}), the cell with $V_{PLC(1)}$=0.015 μM s^{-1} cannot show [Ca^{2+}] oscillations, i.e., N=0.

We have demonstrated that the gradient of V_{PLC} ($\Delta V_{PLC}=V_{PLC(2)}-\Delta V_{PLC(1)}$) can change the effects of coupling strength γ_{IP}. In Fig. 12, with the increase of ΔV_{PLC}, the ratio of N/M decreases with a staircase-like structure.

The phase diagram in two-dimensional parameter space of the coupling strength IP and $V_{PLC(1)}$ has been predicted in Fig. 13, which is similar to Fig. 6. The method to define the synchronous and nonsynchronous behavior is the same as the method in Fig. 6.

4. Conclusions

In this article, basing on Höfer 's model and employing the Li–Rinzel model to describe the receptor flux, we have explored theoretically the intercellular Ca^{2+} oscillations in coupled hepatocytes. Coupled hepatocytes are connected by gap junctions, which can be permeable to Ca^{2+} and to IP_3. Therefore, we have studied the effects of two coupling strength (γ_{CA} and γ_{IP}) on the synchronization of a pair of coupled cells. In particular, the effects of the intracellular IP_3 level and of the velocity of IP_3 synthesis have also been studied.

By comparing bifurcation diagrams of the isolated cell and of two coupled cells (Figs. 1 and 8), it has been found that, although the oscillation range for coupled cells is larger than the one for isolated cell, the [Ca^{2+}] in coupled cells is lower than that in the isolated cell when IP_3 level is high. An interesting extrapolation of our results is that communication between cells can sometimes avoid fatally high concentration of intracellular Ca^{2+}.

The frequency of [Ca^{2+}] oscillations elicited by a given agonist concentration differs between individual hepatocytes [21,7]. However, in multicellular systems of rat hepatocytes [25,28] and even in the intact liver [12,11], [Ca^{2+}] oscillations are synchronized and highly coordinated. This fact is well confirmed in our results.

A peculiar feature of intercellular Ca^{2+} waves in hepatocytes, compared with other cell types, is that they require the continuous presence of an agonist [13]. Figs. 3 and 10 demonstrate that sufficient and continuous IP_3 level is necessary for the synchronization of IP_3-induced [Ca^{2+}] oscillations in coupled hepatocytes.

Besides [Ca^{2+}] in coupled hepatocytes showing phase-locking oscillations, it can also exhibit a diversity of harmonic locking for different coupling strength and IP_3 level (Figs. 4, 5, 11 and 12). This suggests that coupling strength and IP_3 level play important roles in the synchronization of [Ca^{2+}] oscillations in coupled hepatocytes.

To clearly characterize the effects of coupling strength and IP_3 level on synchronization of intercellular [Ca^{2+}] oscillations, we predict the phase diagram in P–γ_{CA} parameter space, in which the synchronization region is similar to Arnol'd tongue.

Finally, Cross-correlation analysis in Fig. 7 suggests that there exist optimal coupling strength and IP_3 stimulus for the synchronization of intercellular [Ca^{2+}] oscillations.

However, there is still some limitations in this model. For example, the relative constancy of the calcium oscillations amplitude is not reproduced in this paper. As mentioned in the Introduction, stochastic modelling of [Ca^{2+}] oscillations can obtain a better explanation of experimental results. Considering that stochastic fluctuation of [Ca^{2+}] might impose on the synchronization of intercellular Ca^{2+}oscillations, we will study a stochastic version of the above model in future work.

Acknowledgments

This work was supported by the National Natural Science Foundation of China under Grant No. 10275026.

References

[1] A. Goldbeter, Biochemical Oscillations and Cellular Rhythms. The Molecular Bases of Periodic and Chaotic Behaviour, Cambridge Univ. Press, Cambridge, 1996.

[2] M.J. Berridge, Inositol trisphosphate and calcium signalling, Nature 361 (1993) 315–325.

[3] O.H. Petersen, C.C.H. Petersen, H. Kasai, Cacium and hormone action, Annu. Rev. Physiol. 56 (1994) 297–319.

[4] T. Pozan, R. Rizzuto, P. Volpe, J. Meldolesi, Molecular and cellular physiology of intracellular calcium stores, Physiol. Rev. 74 (1994) 595–636.

[5] A.P. Thomas, G.S.J. Bird, G. Hajnoczky, L.D. Robbgaspers, J.W. Putney, Spatial and temporal aspects of cellular calcium signaling, FASEB. J. 10 (1996) 1505–1517.

[6] N.M. Woods, K.S.R. Cuthberon, P.H. Cobbold, Repetitive transient rises in cytoplasmic free calcium in hormone-stimulated hepatocytes, Nature 319 (1986) 600–602.

[7] T.A. Rooney, E.J. Sass, A.P. Thomas, Characterization of cytosolic calcium oscillations induced by phenylephrine and vasopressin in single fura-2-loaded hepatocytes, J. Biol. Chem. 264 (1989) 17131–17141.

[8] D. Wu, Y. Jia, A. Rozi, Effects of inositol 1,4,5-trisphosphate receptor-mediated intracellular stochastic calcium oscillations on activation of glycogen phosphorylase, Biophys. Chem. 110 (2004) 179–190.

[9] A. Rozi, Y. Jia, A theoretical study of effects of cytosolic Ca^{2+} oscillations on activation of glycogen phosphorylase, Biophys. Chem. 106 (2003) 193–202.

[10] H. Kasai, O.H. Petersen, Spatial dynamics of second messengers: IP_3 cAMP as long-range and associative messengers, Trends Neurosci. 17 (1994) 95–101.

[11] L.D. Robbgaspers, A.P. Thomas, Coordination of Ca^{2+} signaling by intercellular propagation of Ca^{2+} waves in the intact liver, J. Biol. Chem. 270 (1995) 8102–8107.

[12] M.H. Nathanson, A.D. Burgstahler, A. Mennone, M.B. Fallon, C.B. Gonzalez, J.C. Sáez, Ca^{2+} waves are organized among hepatocytes in the intact organ, Am. J. Physiol. 32 (1995) G167–G171.

[13] T. Tordjmann, B. Berthon, M. Claret, L. Combettes, Coordinated intercellular calcium waves induced by noradrenaline in rat hepatocytes: dual control by gap junction permeability and agonist, EMBO J. 16 (1997) 5398–5407.

[14] T. Tordjmann, B. Berthon, E. Jacquemin, C. Clair, N. Stelly, G. Guillon, M. Claret, L. Combettes, Receptor-oriented intercellular waves evoked by vasopressin in rat hepatocytes, EMBO. J. 17 (1998) 4695–4703.

[15] G. Dupont, T. Tordjmann, C. Clair, S. Swillens, M. Claret, L. Combettes, Mechanism of receptor-oriented intercellular calcium wave propagation in hepatocytes, FASEB. J. 14 (2000) 279–289.

[16] Th. Höfer, Model of intercellular calcium oscillations in hepatocytes: synchronization of heterogeneous cells, Biophys. J. 77 (1999) 1244–1256.

[17] M.E. Gracheva, R. Toral, J.D. Gunton, Stochastic effects in intercellular calcium spiking in hepatocytes, J. Theor. Biol. 212 (2001) 111–125.

[18] G.W. De Young, J. Keizer, A single-pool inositol 1,4,5-triphosphate-receptor-based model for agonist-stimulated oscillations in Ca^{2+} concentration, Proc. Natl. Acad. Sci. U. S. A. 89 (1992) 9895–9899.

[19] Y. Li, J. Rinzel, Equations for $InsP_3$ receptor-mediated $[Ca^{2+}]_i$ oscillations derived from a detailed kinetic model: a Hodgkin–Huxley like formalism, J. Theor. Biol. 166 (1994) 461–473.

[20] G. Dupont, C. Erneux, Simulations of the effects of inositol 1,4,5-trisphosphate 3-kinase and 5-phosphatase on Ca^{2+} oscillations, Cell Calcium 22 (1997) 321–331.

[21] T. Kawanishi, L.M. Blank, A.T. Harootunian, M.T. Smith, R.Y. Tsien, Ca^{2+} oscillations induced by hormonal stimulation of individual fura-2-loaded hepatocytes, J. Biol. Chem. 264 (1989) 12859–12866.

[22] P. Parmananda, C.H. Mena, G. Baier, Resonant forcing of a silent Hodgkin–Huxley neuron, Phys. Rev. E. 66 (2002) 047202.

[23] A.S. Pikovsky, J. Soviet, Phase synchronization of chaotic oscillations by a periodic external field, Commun. Technol. Electron. 30 (1985) 1970–1974.

[24] A.S. Pikovsky, M. Rosenblum, J. Kurths, Phase synchronization of chaotic oscillators by external driving, Physica (Amsterdam) D 140 (1997) 219–238.

[25] M.H. Nathanson, A.D. Burgstahler, Coordination of hormone induced calcium signals in isolated rat hepatocyte couplets—demonstration with confocal mocroscopy, Mol. Biol. Cell 3 (1992) 113–121.

[26] N.L. Ostrowski, W.S. Young, M.A. Knepper, S.J. Lolait, Expression of vasopressin VIa and V2 receptor messenger ribonucleic acid in the liver and kidney of embryonic, developing, and adult rats, Endocrinology 133 (1993) 1849–1859.

[27] T. Tordjmann, B. Berthon, L. Combettes, M. Claret, The location of hepatocytes in the rat liver acinus determines their sensitivity to calcium-mobilizing hormones, Gastroenterology 111 (1996) 1343–1352.

[28] L. Combettes, D. Tran, T. Tordjmann, M. Laurent, B. Berthon, M. Claret, Ca^{2+}-mobilizing hormones induce sequentially ordered Ca^{2+} signals in multicellular systems of rat hepatocytes, Biochem. J. 304 (1994) 585–594.